



Research Note

Holographic lens for 532 nm in photo-thermo-refractive glass

Fedor Kompan^{a,*}, Ivan Divliansky^a, Vadim Smirnov^b, Leonid Glebov^{a,b}^a CREOL the College of Optics and Photonics, University of Central Florida, Orlando, FL 32816, USA^b OptiGrate Corporation, 562 S. Econ Circle, Oviedo, FL 32765, USA

ARTICLE INFO

Article history:

Received 10 November 2017

Received in revised form 7 February 2018

Accepted 21 February 2018

Keywords:

Volume Bragg gratings

Photo-thermo-refractive glass

Complex holograms

Holographic optical elements

Laser beam control

ABSTRACT

Volume Bragg gratings (VBGs) recorded in photo-thermo-refractive (PTR) glass are extensively used for laser beam control applications. As planar holographic optical elements, VBGs operate in the entire spectral window of PTR glass transparency – from near UV, through visible, and up to IR spectral regions. However, complex holographic elements, e.g. lenses or curved mirrors, cannot be fabricated in conventional Ce³⁺ doped PTR glass for applications in the visible spectral region due to its photosensitivity being limited to the UV region. Recently developed PTR glass doped with Tb³⁺ ions demonstrated sensitivity to visible light. The photo-ionization involves two-step absorption of UV and visible photons via metastable levels of Tb³⁺. Holograms in this glass were recorded by simultaneous exposure to UV radiation from an LED and visible radiation of the second harmonic from a Nd:YAG laser at 532 nm. For the first time holographic lenses operating at 532 nm were demonstrated in PTR glass. This result paves the way for complex holographic optical elements for operation with high power visible lasers.

© 2018 Elsevier Ltd. All rights reserved.

1. Introduction

Optical elements produced by means of holographic recording are known as holographic optical elements (HOEs). Such optical elements can perform as spatial or spectral filters, lenses, mirrors, diffraction gratings, prisms, or beam splitters [1]. It might be often beneficial to employ an HOE in optical systems, as holographic structures possess several advantages over conventional optical elements [2]. The advantages include relatively low production cost, reproducibility, multiplexing, and most importantly, wavelength selectivity. Besides, HOEs tend to have smaller size and flat surfaces allowing for reduction of the dimensions of the entire optical system.

1.1. Applications of holographic optical elements

The advantages described above give rise to a variety of applications for the HOEs, where visible light applications are found to be highly demanded [2,3]. For example, light detection and ranging systems (LIDARS) for atmosphere sensing use a probe laser beam, typically at the wavelength of 532 nm, for scanning of the atmosphere [4]. The laser light reflected from different areas of the atmosphere is then collected by a primary curved mirror of a telescope, spectrally filtered, and focused by a secondary curved mirror

to a detector. However, regardless of conventional spectral filtering, a substantial amount of background radiation might be collected by the telescope along with the desired signal due to the large bandwidth of the optical filters included in the system if compared to the bandwidth of a single frequency probe laser beam. This problem can be resolved by replacing the focusing mirror with its holographic counterpart. The filtering capabilities of the holographic mirror would provide an opportunity to detect radiation only at the desired wavelength by focusing only the desired wavelengths to the detector and thus substantially increasing the signal to noise ratio. Other visible light applications include RGB light combiners, head mounted displays for pilots [5], fiber optic couplers, wavelength multiplexers and demultiplexers as well as other applications [3].

1.2. Photo-thermo-refractive glass for recording of holographic optical elements

Performance of an HOE depends largely on the properties of the holographic material in which the hologram is fabricated. Many applications of an HOE such as LIDAR require a material with high photosensitivity, high spatial resolution, low scattering, and tolerance to high-power laser radiation. Conventional holographic materials with visible photosensitivity such as dichromated gelatin (DCG), silver halide photoemulsions, and doped lithium niobate are mostly unsuitable as none of them provides all the desired properties combined [6–8]. A photosensitive glass such as

* Corresponding author.

E-mail address: fedor.kompan@knights.ucf.edu (F. Kompan).

photo-thermo-refractive (PTR) glass allows overcoming the constraints of the materials mentioned above. PTR glass is a $\text{Na}_2\text{O-ZnO-Al}_2\text{O}_3\text{-SiO}_2$ silicate glass doped with Ce^{3+} , Ag^+ , Sn^{4+} and Sb^{5+} [9,10]. The glass is widely used for the fabrication of HOEs such as volume Bragg gratings (VBGs) [11–15] and phase masks [16]. A hologram in PTR glass is fabricated by two stage process including exposure to UV radiation and thermal treatment. The exposure to UV radiation creates a latent image. Refractive index modulation (RIM) is produced during a thermal development stage. The refractive index change obtained using this procedure is permanent, and cannot be subsequently altered [17,18]. Holograms produced in PTR glass are volume gratings recorded in the bulk of a glass sample as opposed to conventional surface gratings and because of this at resonance they exhibit single diffraction order. In addition, VBGs recorded in PTR glass can also handle high-power laser radiation. For example, a VBG recorded in PTR glass did not demonstrate any significant performance degradation upon illumination by a CW laser beam (at 1 μm wavelength) with power density close to 100 kW/cm^2 [19].

1.3. Shortcomings of the regular photo-thermo-refractive glass

Planar holographic optical elements in PTR glass are recorded using UV light and can operate in the entire spectral window of PTR glass transparency – from near UV, through visible, and up to IR spectral regions. However, a complex HOE fabrication process imposes an important requirement, which states that the readout wavelength should match the wavelength of radiation used for recording of the hologram [20]. Therefore, a complex hologram designed for applications in the visible spectral region would operate when recorded using the corresponding visible radiation. Conventional Ce^{3+} doped PTR glass does not allow for recording using visible radiation since its photosensitivity range is limited to the UV region between 280 and 350 nm. Therefore, planar gratings are the only type of optical elements, which can be produced in a conventional PTR glass for applications beyond the UV region.

2. Experimental

A new PTR glass with a different photosensitizer – Tb^{3+} (Tb:PTRG^1) was recently developed [21]. The photosensitivity mechanism in Tb:PTRG is based on excited state absorption (ESA) upconversion process [22]. Absorption of a near UV photon results in electron excitation from the ground state to the upper $^5\text{D}_3$ level of the Tb^{3+} ion (Fig. 1) followed by a nonradiative relaxation to the lower $^5\text{D}_4$ level. The $^5\text{D}_4$ level is metastable. A subsequent absorption of visible photons results in excitation of the 5d band, which is located above the electron mobility threshold in Tb:PTRG [21]. Therefore, Tb^{3+} ion is converted to a Tb^{4+} ion, releasing an electron, which is finally captured by a silver ion Ag^+ triggering structural transformations similar to those in conventional PTR glass that eventually result in negative refractive index change in the exposed areas [9]. This feature of Tb:PTRG provided a potential for hologram recording with simultaneous exposure of the glass to a spatially uniform UV beam (pump) and a patterned visible beam (recording by interference of reference and signal beams).

2.1. Optimization of Tb^{3+} doped photo-thermo-refractive glass for holographic applications

However, real holographic applications were hindered by the low photosensitivity of the Tb:PTRG resulting in relatively small RIM as well as fairly long recording times. In the present work,

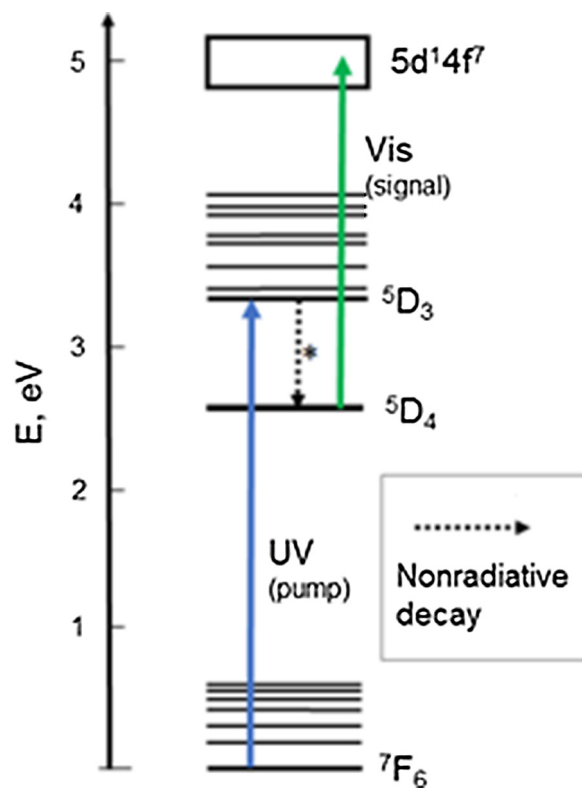


Fig. 1. Energy levels of Tb^{3+} [21]. Scheme of excited state absorption shown by arrows.

the photosensitivity of the glass was optimized which made holographic recordings possible. In particular, such factors as exposure dosages of the UV and the visible radiation as well as their intensity ratio were optimized along with the parameters of the thermal development procedure. During our previous experiments, the longest wavelength at which photosensitivity of the Tb:PTRG was observed was 522 nm by using a concurrent irradiation by a CW LED operating at 375 nm with power density of approximately 1 W/cm^2 and a CW laser diode operating at 522 nm with power density of about 40 W/cm^2 [21]. The obtained refractive index change was close to 200 ppm. In this paper, the 532 nm laser line was chosen as a signal source due to the larger excited state absorption of the glass in that part of the spectrum as well as because of the abundance of laser sources available at this wavelength. Subsequent experiments were carried out using two light sources. A UV pump source provided the primary excitation via ground state absorption, and a visible recording source provided further excitation from the metastable level (Fig. 1). The same UV LED as in Ref. [21] delivering 450 mW of power at 375 nm was used as a pump source. Subsequent ESA was implemented by means of a high irradiance nanosecond laser delivering 200 mJ energy pulses at 532 nm with peak power density of 45 MW/cm^2 and repetition rate of 20 Hz. The photosensitivity (difference of refractive indices between exposed and unexposed areas) of Tb:PTRG exposed to a Gaussian stripe at 532 nm on a background of a uniform beam at 375 nm was measured with a shearing interferometer [23]. It was found that the glass is photosensitive when simultaneously exposed to 532 and 375 nm radiation. The dependence of the RIM from different dosages of pulsed (10 ns) radiation at 532 nm and for different power densities is shown in Fig. 2. The refractive index change increases with the dosage reaching saturation of near 400 ppm at approximately 30 kJ/cm^2 . This value is close to two times higher than that observed in Ref. [21]. It is clear that the efficiency of the excited state absorption process depends on the

¹ Tb:PTRG – Tb^{3+} doped photo-thermo-refractive glass.

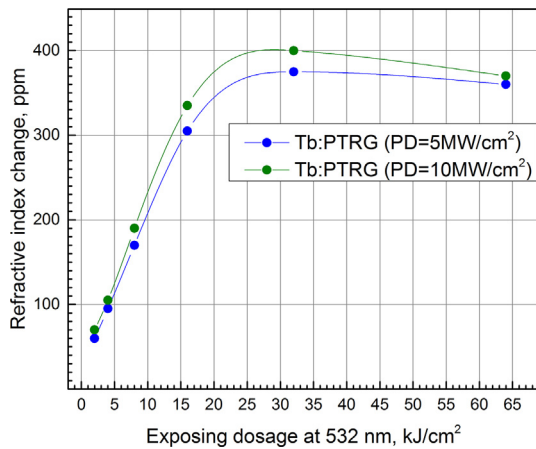


Fig. 2. Refractive index change in Tb³⁺ doped PTR glass after concurrent exposure to 10 ns laser pulses at 532 nm and CW LED beam at 375 nm; two curves correspond to different peak power densities (PD) for a 532 nm beam.

power densities of the UV and visible light. The first one determines the concentration of electrons at the metastable level while the second one determines the excitation rate from the metastable level to the 5d band. A supposition could be made, that the higher power density in these experiments is responsible for higher refractive index change when compared to the results observed in Ref. [21]. One can see in Fig. 2 that the refractive index changes for 5 and 10 MW/cm² are similar because these power densities provide complete excitation of the electrons from the metastable level. The RIM would decrease if the power density of visible radiation is decreased below 5 MW/cm².

3. Results and discussion

To demonstrate the feasibility of visible hologram recording in Tb:PTRG, a simple transmitting VBG was recorded first. A high irradiance laser with long coherence length operating at 532 nm, outlined in Section 2.1, was used as a source. The laser was specifically designed for holographic purposes and featured injection seeding technology providing close to transform limited pulses as well as frequency stability. A collimated 532 nm beam was equally split by a beamsplitter creating the signal and the reference beams that were combined at a full convergence angle of 6°. The resulting interference pattern had a period of 5 μm. A Tb:PTRG plate was placed at the intersection of the two beams. The sample was simultaneously exposed to the interfering visible beams and a UV pump beam incident from the backside of the sample. Modeling has shown that 2 mm thick Tb:PTRG plate should have refractive index modulation of 130 ppm to provide 99.99% diffraction efficiency. To achieve this RIM, exposure dosages of 32 kJ/cm² for the visible radiation and 1 kJ/cm² for the UV radiation. The subsequent thermal development of the glass sample was carried out for 100 min at 525 °C. The recorded VBG had diffraction efficiency of 91%. It is believed that the difference between the expected and the observed values is a result of smearing of the interference fringes due to setup instabilities [24].

3.1. Holographic lens in Tb³⁺ doped photo-thermo-refractive glass

As a next experiment, a hologram of a positive convex lens operating at 532 nm was recorded in a Tb:PTRG plate. The recording setup used for the purpose is shown in Fig. 3. A collimated beam of a pulsed laser at 532 nm was split to reference and signal beams. The collimated signal beam was converted to a divergent

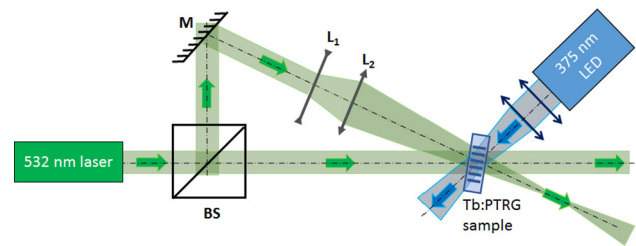


Fig. 3. Experimental setup for recording holographic lens in Tb³⁺ doped PTR glass (BS – beamsplitter, M – mirror, L₁, L₂ – lenses).

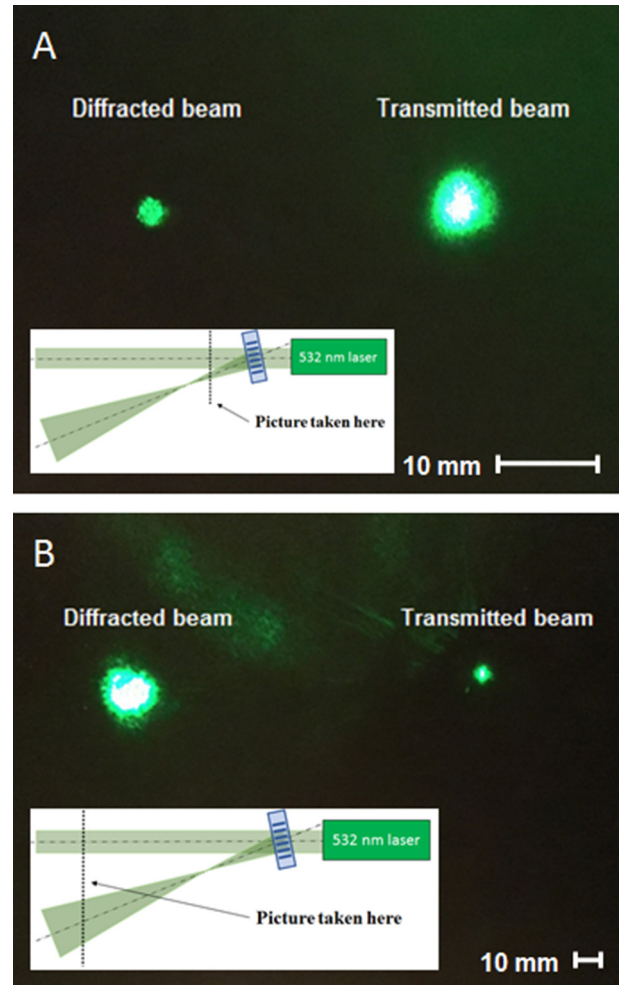


Fig. 4. Photos of beams diffracted and transmitted through a holographic lens. (A) Transmitted and diffracted beams before the focal plane, (B) transmitted and diffracted beams after focal plane. Photos are taken with different zoom – same transmitted beam size in both pictures.

one by a negative lens. The beam of an increased diameter was then focused by a positive lens to provide equal diameters of the signal and reference beams in the recording plane. A glass plate was placed at the intersection of the recording beams whereas pumping was provided by illuminating the sample from the backside by a beam from the UV LED. Afterwards, the exposed glass plate underwent a standard thermal development.

When the developed glass sample was illuminated by a collimated beam from the 532 nm laser under the same angle to the surface normal as in the recording setup, the incident beam was diffracted and focused by the hologram. The operation of the holo-

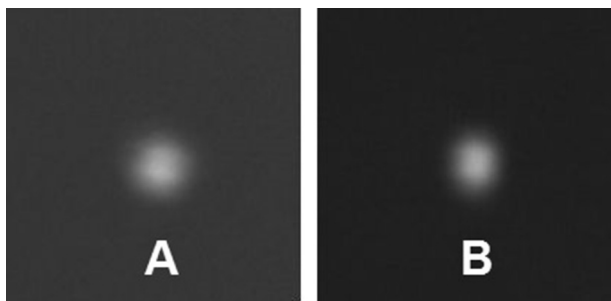


Fig. 5. Photos of spots in focal plane of original lens system (A) and holographic lens (B).

graphic lens as a focusing element is demonstrated in Fig. 4. The diffracted beam converges as it emerges from the hologram and its size becomes smaller compared to the transmitted collimated beam (Fig. 4a). As the diffracted beam propagates, it passes through its minimum size at the focal plane and then starts to diverge. It can be seen from Fig. 4b that its size eventually exceeds that of the collimated transmitted beam. The holographic lens showed the diffraction efficiency of 90%. Similarly to the transmitting VBG described earlier, the difference is due smearing of the interference fringes during recording procedure. It is believed that the efficiency could be improved to match the target value of 99.99% by introducing an active phase stabilization system [25,26]. It should be mentioned that rotating the holographic lens by 180° in the plane of Fig. 4 converts it to a negative lens defocusing the collimated test beam.

3.2. Imaging performance of holographic lens

The imaging performance of the holographic lens is of utmost importance as it determines whether an HOE can be an equivalent substitute for its alternatives. The main concern is that aberrations might be introduced by the HOE into the diffracted beam. Detailed aberration analysis is beyond the scope of this paper and will be carried out in the future. However, the minimum beam spot size was measured in the focal plane of both original and holographic lenses. Fig. 5 demonstrates images of the beams in the focal plane of the original lens system (A) and the holographic lens (B). The RMS spot size underwent only a slight increase from 250 μm in the original lens system (a combination of negative and positive lenses) to 270 μm for the hologram. It can be inferred that the imaging performance of the complex conventional lens system is almost completely reproduced by the holographic lens.

4. Conclusions

In conclusion, a new Tb³⁺ doped PTR glass demonstrated refractive index change after simultaneous illumination by 375 nm

(pumping) and 532 nm (recording) beams and enabled fabrication of complex HOEs operating in the visible spectrum. Refractive index change of 400 ppm was observed. This value enables recording of volume holographic optical elements with 100% diffraction efficiency. Planar volume Bragg gratings and holographic lens operating at 532 nm were demonstrated. Both types of transmitting holograms showed the diffraction efficiency of 90% or higher.

Acknowledgements

Authors thank L. Glebova and H. Mingareev for the design and the fabrication of Tb³⁺ doped PTR glass.

References

- [1] R. Collier, C.B. Buckart, L.H. Lin, *Optical Holography*, Academic, New York, 1971.
- [2] K. Schwartz, *The Physics of Optical Recording*, Springer-Verlag, Heidelberg, Germany, 1993.
- [3] D.H. Close, *Optically Recorded Holographic Optical Elements*, Handbook of Optical Holography, Academic Press, New York, 1979.
- [4] G.K. Schwemmer, R.D. Rallison, T.D. Wilkerson, D.V. Guerra, *Opt. Lasers Eng.* 44 (2006) 881.
- [5] F. Dimov, T. Aye, K. Yu, S. Soboleva, K. S. Yin, M. Kyaw, D. Voloschenko US Patent 20100157400 A1, issued 2009.
- [6] B.J. Chang, C.D. Leonard, *Appl. Opt.* 18 (1979) 2407.
- [7] I. Naydenova, V. Toal, *Nanoparticle doped photopolymers for holographic applications*, in: V. Valtchev, S. Mintova, M. Tsapatsis (Eds.), *Ordered porous Solids*, Elsevier, 2008.
- [8] D.K. McMillen, T.D. Hudson, J. Wagner, J. Singleton, *Opt. Express* 2 (1998) 491.
- [9] L.B. Glebov, N.V. Nikonorov, E.I. Panysheva, G.T. Petrovskii, V.V. Savvin, I.V. Tunimanova, V.A. Tsekhomskii, *Polychromatic glasses – a new material for recording volume phase holograms*, *Sov. Phys. Dokl.* 35 (10) (1990) 878–880.
- [10] L.B. Glebov, *Photochromic and photo-thermo-refractive (PTR) glasses*, in: M. Schwartz (Ed.), *Encyclopedia of Smart Materials*, John Wiley & Sons, NY, 2002.
- [11] L.B. Glebov, *J. Holography Speckle* 5 (2008) 1.
- [12] O. Andrusyak, V. Smirnov, G. Venus, V. Rotar, L. Glebov, *IEEE J. Select. Top. Quantum Electron.* 15 (2009) 344.
- [13] A.L. Glebov, O. Mokhun, A. Rapaport, S. Vergnole, V. Smirnov, L.B. Glebov, *Proc. SPIE* 8428 (2012) 1.
- [14] L. Glebov, *Rev. Laser Eng.* 41 (2013) 684.
- [15] L. Glebov, V. Smirnov, E. Rotari, I. Cohanoschi, L. Glebova, O. Smolski, J. Lumeau, C. Lantigua, A. Glebov, *Opt. Eng.* 53 (2014) 1.
- [16] M. SeGall, I. Divliansky, C. Jollivet, A. Schülzgen, L.B. Glebov, *Opt. Eng.* 54 (2015) 1.
- [17] L.B. Glebov, V.I. Smirnov, C.M. Stickley, I.V. Ciapurin, *Proc. SPIE* 4724 (2002) 101.
- [18] N.V. Nikonorov, E.I. Panysheva, I.V. Tunimanova, A.V. Chukharev, *Influence of glass composition on the refractive index change upon photothermoinduced crystallization*, *Glass Phys. Chem.* 27 (3) (2001) 241–249.
- [19] I.V. Ciapurin, L.B. Glebov, L.N. Glebova, V.I. Smirnov, E.V. Rotari, *Proc. SPIE* 4979 (2003) 209.
- [20] R. Syms, *Practical Volume Holography*, Oxford University Press, 1990.
- [21] F. Kompan, G. Venus, L. Glebova, H. Mingareev, L. Glebov, *Opt. Mater. Express* 6 (2016) 3881.
- [22] F. Auzel, *Chem. Rev.* 104 (2004) 1864.
- [23] O.M. Efimov, L.B. Glebov, H.P. Andre, *Appl. Opt.* 41 (2002) 1864.
- [24] D. Ott, V.K. Rotaru, J. Lumeau, S. Mokhov, I.B. Divliansky, A.I. Rysanyanskiy, N. Vorobiev, V. Smirnov, C. Spiegelberg, L.B. Glebov, *Proc. SPIE* 8236 (2012) 823621.
- [25] D.R. MacQuigg, *Hologram fringe stabilization method*, *Appl. Opt.* 16 (1977) 291–292.
- [26] D.B. Ott, I.B. Divliansky, M.A. SeGall, L.B. Glebov, *Appl. Opt.* 53 (2014) 1039.